Haplo-Insufficiency of *MPK3* in *MPK6* Mutant Background Uncovers a Novel Function of These Two MAPKs in *Arabidopsis* Ovule Development [W]

Huachun Wang,[a] Yidong Liu,[a] Kristin Bruffett,[a] Justin Lee,[b] Gerd Hause,[c] John C. Walker,[d] and Shuqun Zhang[a,1]

[a] Department of Biochemistry and Bond Life Sciences Center, University of Missouri, Columbia, Missouri, 65211
[b] Leibniz Institute of Plant Biochemistry, D-06120, Halle, Germany
[c] Biocenter of the University of Halle, D-06120, Halle, Germany
[d] Division of Biological Sciences and Bond Life Sciences Center, University of Missouri, Columbia, Missouri, 65211

The plant life cycle includes diploid sporophytic and haploid gametophytic generations. Female gametophytes (embryo sacs) in higher plants are embedded in specialized sporophytic structures (ovules). Here, we report that two closely related mitogen-activated protein kinases in *Arabidopsis thaliana*, MPK3 and MPK6, share a novel function in ovule development: in the *MPK6* mutant background, *MPK3* is haplo-insufficient, giving female sterility when heterozygous. By contrast, in the *MPK3* mutant background, MPK6 does not show haplo-insufficiency. Using wounding treatment, we discovered gene dosage–dependent activation of MPK3 and MPK6. In addition, MPK6 activation is enhanced when MPK3 is null, which may help explain why $mpk3^{-/-}$ $mpk6^{+/-}$ plants are fertile. Genetic analysis revealed that the female sterility of $mpk3^{+/-}$ $mpk6^{-/-}$ plants is a sporophytic effect. In $mpk3^{+/-}$ $mpk6^{-/-}$ mutant plants, megasporogenesis and megagametogenesis are normal and the female gametophyte identity is correctly established. Further analysis demonstrates that the $mpk3^{+/-}$ $mpk6^{-/-}$ ovules have abnormal integument development with arrested cell divisions at later stages. The mutant integuments fail to accommodate the developing embryo sac, resulting in the embryo sacs being physically restricted and female reproductive failure. Our results highlight an essential function of MPK3 and MPK6 in promoting cell division in the integument specifically during ovule development.

INTRODUCTION

The life cycle of plants includes a diploid sporophytic generation and a haploid gametophytic generation. In angiosperms, including *Arabidopsis thaliana*, the sporophyte is the predominant free-living generation, whereas the gametophytic phase is dependent on and embedded in sporophytic structures called ovules. The *Arabidopsis* ovule comprises the distal nucellus, central chalaza, and the proximal funiculus along the distal-proximal axis. The nucellus harbors the megaspore mother cell (MMC), which undergoes meiosis and subsequently gives rise to the female gametophyte. The inner and outer integuments initiate from the central chalaza and eventually envelop the nucellus. The integuments will develop into the seed coat after fertilization to protect the developing embryo. The proximal funiculus connects the ovule with the sporophytic tissue and is believed to channel nutrients to the developing ovule (Misra, 1962; Schneitz et al., 1995).

The development of female gametophytes needs to be coordinated with the surrounding sporophytic integuments (Yang and Sundaresan, 2000; Acosta-Garcia and Vielle-Calzada, 2004;

Yadegari and Drews, 2004). Sporophytic tissues are believed to be responsible for the establishment of polarity within the female gametophyte (Huang and Russell, 1992; Christensen et al., 1997; Yadegari and Drews, 2004). The presence of plasmodesmata connecting the developing female gametophyte with the neighboring nucellar cells indicates that cell–cell interactions are important for the female gametophyte development (Bajon et al., 1999). Mutants with defective integument initiation and outgrowth, such as *ant* (an AP2 transcription factor), *ino* (*INNER NO OUTER*, a YABBY transcription factor), *bel1* (*BELL1*, a homeodomain transcription factor), *tsl* (*TOUSLED*, a nuclear Ser/Thr protein kinase), and *sin1/dcl1* (*SHORT INTEGUMENTS1/DICER LIKE1*, a ribonuclease), are associated with aborted embryo sac development (Robinson-Beers et al., 1992; Ray et al., 1994; Reiser et al., 1995; Elliott et al., 1996; Klucher et al., 1996; Roe et al., 1997; Villanueva et al., 1999; Golden et al., 2002; Meister et al., 2002). On the one hand, these observations suggest that coordinated development between the developing embryo sac and the surrounding sporophytic tissues is crucial for female fertility. On the other hand, there are mutants such as *female gametophyte12* (*fem12*) or *fem16* in which the embryo sac aborts at early development stages, but the ovule integument development is almost normal, suggesting that ovule development is independent of the embryo sac development (Christensen et al., 2002).

Mitogen-activated protein kinase (MAPK) signaling cascades are three-tiered kinase modules that are conserved across all eukaryotes (Ichimura et al., 2002). They function downstream of

sensors/receptors and convert signals generated at the sensors/receptors into cellular responses (Widmann et al., 1999; Chang and Karin, 2001; Schwartz and Madhani, 2004). Each MAPK cascade is composed of three kinases. Phosphorylation activation of MAPKs is performed by MAPK kinases (MAPKKs or MEKs), which are in turn activated by MAPKK kinases (MAPKKKs or MEKKs). In *Arabidopsis*, there are 20 MAPKs, 10 MAPKKs, and ~60 MAPKKKs, among which 12 belong to the MEKK subgroup (Ichimura et al., 2002; Hamel et al., 2006). Emerging evidence indicates that MAPK cascades not only play important functions in regulating stress responses but also function as key regulators of plant growth and development (reviewed in Tena et al., 2001; Zhang and Klessig, 2001; Nakagami et al., 2005; Pedley and Martin, 2005; Wang et al., 2007b).

Here, we report that MPK3 and MPK6 share novel overlapping functions in regulating the development of ovule integuments. Plants that are heterozygous for *mpk3* and homozygous for *mpk6* (*mpk3$^{+/-}$ mpk6$^{-/-}$*) are female sterile due to a sporophytic defect. The haplo-insufficient *mpk3$^{+/-}$ mpk6$^{-/-}$* mutant ovules have abnormal ovule integument development with reduced cell proliferation at the late stage, which results in embryo sacs being physically restricted and female sterility of the *mpk3$^{+/-}$ mpk6$^{-/-}$* mutant plants. These results reveal a novel function of MPK3/MPK6 in regulating the development of ovule integuments, which is critical to accommodate the enlarging embryo sac and formation of functional female reproductive structure.

RESULTS

Haplo-Insuffiency of MPK3 in the MPK6 Mutant Background (*mpk3$^{+/-}$ mpk6$^{-/-}$*) Results in Female Sterility

In an attempt to generate loss-of-function *MPK3* and *MPK6* plants for phenotypic analysis, we found that the *mpk3$^{-/-}$ mpk6$^{-/-}$* double mutant was embryo lethal (Wang et al., 2007a). Interestingly, *mpk3$^{+/-}$ mpk6$^{-/-}$* plants, but not *mpk3$^{-/-}$ mpk6$^{+/-}$* plants, were sterile, although vegetative growth and development were normal in both plants (Figure 1A). The floral structure of *mpk3$^{+/-}$ mpk6$^{-/-}$* plants was normal, with the correct number of sepals, petals, stamens, and carpels (Figure 1B). We have three null mutant alleles of *mpk6*, *mpk6-1*, *mpk6-2*, and *mpk6-3*, and two null mutant alleles of *mpk3*, *mpk3-1* and *mpk3-DG* (Miles et al., 2005; Wang et al., 2007a). All three *mpk6* mutant alleles gave the same female sterile phenotype in either of the two *mpk3$^{+/-}$* mutant allele backgrounds. Results from *mpk3-1* and *mpk6-3* cross were presented in the article. Furthermore, a transgene with a native *MPK6* promoter driving the MPK6 coding sequence (*PMPK6:cMPK6*) could rescue the sterile phenotype of *mpk3$^{+/-}$ mpk6$^{-/-}$* (Figure 1C). These results provided strong evidence that the sterile phenotype in *mpk3$^{+/-}$ mpk6$^{-/-}$* plants is due to the loss of function of *MPK6* and the partial loss of function of *MPK3*.

Reciprocal crosses between *mpk3$^{+/-}$ mpk6$^{-/-}$* and wild-type (*Col-0*) plants were performed to determine the nature of the sterility. Pollination of *mpk3$^{+/-}$ mpk6$^{-/-}$* plants with wild-type pollen grains failed to produce any seeds. Pollination of wild-type plants with pollen grains from *mpk3$^{+/-}$ mpk6$^{-/-}$* plants, however, was successful. Genotyping of the F1 progenies showed that *mpk3$^+$/mpk6$^-$* and *mpk3$^-$/mpk6$^-$* male gametes were transmitted at a 5:1 ratio, instead of a 1:1 ratio ($n = 140$, $\chi^2 = 57.8$, $P < 0.001$). Nonetheless, this result indicates that *mpk3$^+$/mpk6$^-$* and *mpk3$^-$/mpk6$^-$* male gametophytes are both viable, even though they were transmitted at a different efficiency. Pollen viability staining further confirmed that pollen grains from *mpk3$^{+/-}$ mpk6$^{-/-}$* plants had normal morphology and were viable (see Supplemental Figure 1 online), suggesting that the *mpk3$^{+/-}$ mpk6$^{-/-}$* genotype caused female-specific sterility.

The Female Sterility of *mpk3$^{+/-}$ mpk6$^{-/-}$* Plants Is Due to a Sporophytic Effect

To determine if the female sterility of *mpk3$^{+/-}$ mpk6$^{-/-}$* plants is a gametophytic or a sporophytic effect, we pollinated *mpk3$^{-/-}$ mpk6$^{+/-}$* plants, which are fertile, with pollen grains from wild-type plants. Genotyping of the F1 progenies showed that *mpk3$^-$/mpk6$^+$* and *mpk3$^-$/mpk6$^-$* female gametes were transmitted at a 1:1 ratio ($n = 111$, $\chi^2 = 0.45$, $P > 0.5$). This result indicates that *mpk3$^-$/mpk6$^-$* and *mpk3$^-$/mpk6$^+$* female gametophytes are fully viable and that the female-sterile phenotype of *mpk3$^{+/-}$ mpk6$^{-/-}$* plants is due to a sporophytic effect.
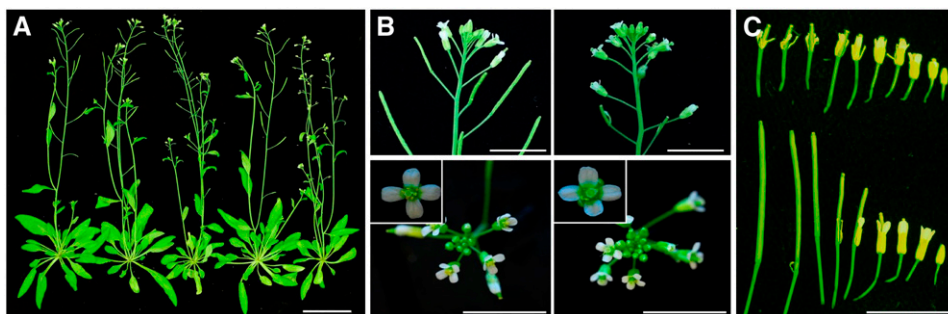

Figure 1. Sterile Phenotype of *mpk3$^{+/-}$ mpk6$^{-/-}$* Plants.

(A) General morphology of the mutants. From left to right: wild type (Col-0), *mpk3$^{-/-}$*, *mpk6$^{-/-}$*, *mpk3$^{-/-}$ mpk6$^{+/-}$*, and *mpk3$^{+/-}$ mpk6$^{-/-}$*. Bar = 5 cm.
(B) Close-up side and top views of the inflorescence. Left panel: wild type; right panel: *mpk3$^{+/-}$mpk6$^{-/-}$*; insets: top views of representative flower.
(C) The *PMPK6:cMPK6* transgene can rescue the sterile phenotype of the *mpk3$^{+/-}$ mpk6$^{-/-}$* mutant. The top row shows the sterile siliques of the *mpk3$^{+/-}$ mpk6$^{-/-}$* mutant, and the bottom row shows the rescued fertile siliques from the *mpk3$^{+/-}$ mpk6$^{-/-}$* plants that carry the *PMPK6:cMPK6* transgene. Bars = 1 cm.

Gene-Dosage Dependent Activation of MPK3 and MPK6

Neither the *mpk3* nor the *mpk6* single null mutant showed a sterile phenotype, indicating that these two MAPKs play an overlapping role in the formation of the functional female reproductive structure. However, the fact that $mpk3^{+/-} mpk6^{-/-}$ but not $mpk3^{-/-} mpk6^{+/-}$ plants are sterile does suggest that they have a differential function in the process. Alternatively, there may be a mechanism to compensate for the loss of one copy of *MPK6* in *mpk3* but not the loss of one copy of *MPK3* in the *mpk6* mutant background. Currently, there is no tool for determining MAPK activation in plant developmental processes, which occurs in a specific tissue or even a few cells. To determine if there is gene-dosage dependent activation of MPK3 and MPK6, we measured the wounding-induced activation of MPK3 and MPK6 in plants with different combinations of genotypes by an in-gel kinase activity assay. As shown in Figure 2, activation of MPK3 was reduced in $mpk3^{+/-}$ plants, regardless of the *MPK6* genotype (lanes 6, 7, 12, and 13). Activation of MPK6 was also reduced in $mpk6^{+/-}$ plants in the $MPK3^{+/+}$ background (lanes 2 and 3). These results suggested that the activation of MPK3 and MPK6 was gene dosage dependent. In addition, wounding activation of MPK6 in $mpk3^{-/-} mpk6^{+/-}$ plants (lanes 10 and 11) was higher than that in $mpk3^{+/+} mpk6^{+/-}$ plants (lanes 2 and 3), suggesting that the activation of MPK3 and MPK6 responds differently when the other MAPK is mutated. There is a mechanism to compensate for missing MPK3 by enhancing the activation of MPK6 but not vice versa. Gene dosage–dependent activation of MPK3 and MPK6 together with the differential compensation at the activation level may help explain the haplo-insufficiency of *MPK3* in the absence of *MPK6*.

Identity Specification and Initiation of Ovule Integuments Are Normal in the $mpk3^{+/-}mpk6^{-/-}$ Plants

To determine the cause of female sterility in $mpk3^{+/-} mpk6^{-/-}$ plants, we examined ovules from wild-type and $mpk3^{+/-} mpk6^{-/-}$ plants at different developmental stages by scanning electron microscopy. Wild-type ovules initiate integuments at stage 2-II (staging according to Schneitz et al., 1995), which begins with the enlargement of epidermal cells at the prospective position of the chalaza. Subsequently, the inner and the outer integument pri-
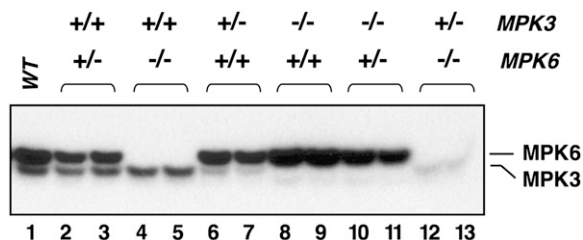

Figure 2. Gene Dosage–Dependent Activation of MPK3/MPK6 and Enhanced Activation of MPK6 in the *mpk3* Mutant in Response to Wounding.

Leaf samples were collected 10 min after wounding. MAPK activation was determined by an in-gel kinase activity assay using myelin basic protein as the substrate. The position of MPK3 and MPK6 bands are labeled in the figure. The faint lowest band is likely due to weak MPK4 activation. Two biological replicates for each genotype were presented.
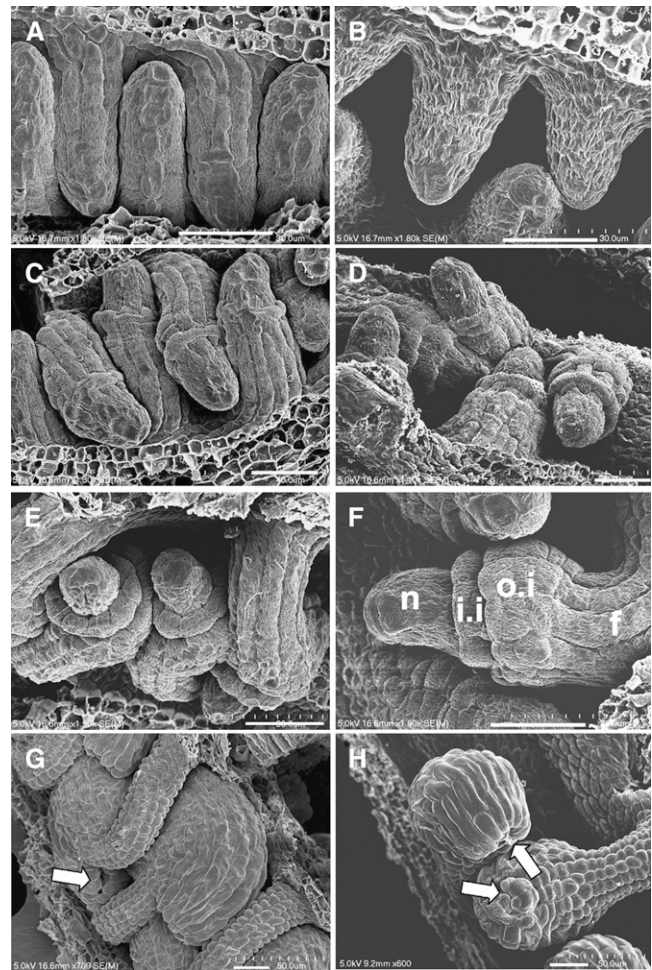

Figure 3. Scanning Electron Micrographs of Ovules from the Wild Type and the $mpk3^{+/-} mpk6^{-/-}$ Mutant.

(A) and **(B)** Ovule primordium outgrowth at stage 2-I.
(C) and **(D)** The initiation of outer and inner integuments at stage 2-III.
(E) and **(F)** The continual outgrowth of nucellus and integuments at stage 2-IV.
(G) By stage 3-VI, wild-type integuments fully enveloped the nucellus and the micropyle was curled around and positioned next to the funiculus.
(H) At stage 3-VI, the integuments from the $mpk3^{+/-} mpk6^{-/-}$ mutant were not able to fully cover the nucellus and the micropylar end was pointed away ~90° from the funiculus.
The wild type is shown in **(A)**, **(C)**, **(E)**, and **(G)**, and the $mpk3^{+/-} mpk6^{-/-}$ mutant is shown in **(B)**, **(D)**, **(F)**, and **(H)**. n, nucellus; i.i, inner integument; o.i, outer integument. Arrows point to the micropyles. Bars = 20 μm.

mordia arise and grow around the nucellus (Figures 3C to 3H). Development of ovules in $mpk3^{+/-} mpk6^{-/-}$ was indistinguishable from that in the wild type at the early stages. The initiation of ovule primodia and the early outgrowth of the inner and outer integuments were relatively normal (cf. stages 2-I and 2-III, Figures 3A to 3D). However, the subsequent growth of ovule integuments in $mpk3^{+/-} mpk6^{-/-}$ was slower than that in the wild type (Figures 3E and 3F). The differences between $mpk3^{+/-} mpk6^{-/-}$ and wild-type ovules became obvious by stage 3-VI. In the wild-type

ovules, the nucellus was fully enveloped by integuments and the micropylar end curled around and was located close to the funiculus (Figure 3G). In the $mpk3^{+/-}$ $mpk6^{-/-}$ ovules, the micropylar end did not bend as far as in the wild type and the integuments did not elongate enough to cover the nucellus (Figure 3H).

Mutants with defects in integument initiation or identity specification are often associated with aborted embryo sac and female sterility (Robinson-Beers et al., 1992; Ray et al., 1994; Reiser et al., 1995; Elliott et al., 1996; Klucher et al., 1996; Villanueva et al., 1999; Golden et al., 2002). To check if there are any defects associated with integument initiation or integument identity specification, we examined *ANT* and *INO* expression patterns in both wild-type and $mpk3^{+/-}$ $mpk6^{-/-}$ ovules by in situ RNA hybridization. In the wild type, *ANT* is expressed in the chalaza at the time of integument initiation and *INO* is expressed in the primodia of the outer integuments (Elliott et al., 1996; Villanueva et al., 1999) (Figures 4A and 4C). The *ANT* and *INO* expression patterns in $mpk3^{+/-}$ $mpk6^{-/-}$ were indistinguishable from that in the wild type, suggesting that both the chalaza and the integuments identities were correctly specified in the $mpk3^{+/-}$ $mpk6^{-/-}$ ovules (Figures 4B and 4D). This result suggests that there is no defect in integument initiation or identity specification in the ovules of $mpk3^{+/-}$ $mpk6^{-/-}$ plants.

Megasporogenesis and Megagametogenesis Are Normal in $mpk3^{+/-}$ $mpk6^{-/-}$ Plants

Female gametophyte development involves two phases: megasporogenesis and megagametogenesis. During megasporogenesis, the MMC enlarges and undergoes meiosis, resulting in the formation of a tetrad (Misra, 1962; Schneitz et al., 1995). In
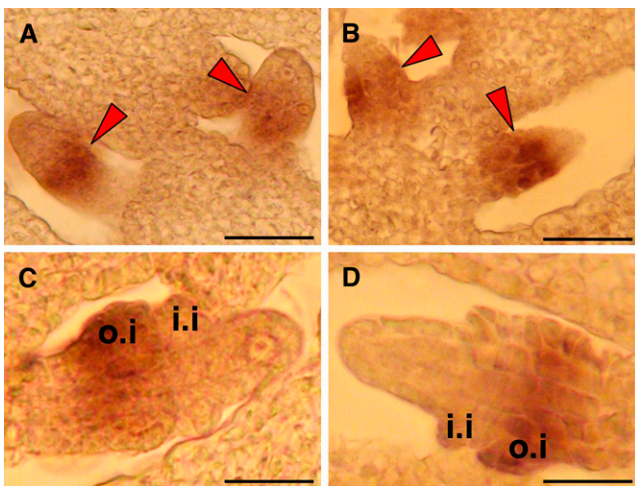

Figure 4. Localization of *ANT* and *INO* by RNA in Situ Hybridization.

(A) and **(B)** *ANT* expression pattern in the wild type **(A)** and the $mpk3^{+/-}$ $mpk6^{-/-}$ mutant ovules **(B)**.
(C) and **(D)** Expression pattern of *INO* in the wild type **(C)** and the $mpk3^{+/-}$ $mpk6^{-/-}$ mutant ovules **(D)**. Sections were probed with *ANT* or *INO* antisense probe, respectively. i.i, inner integument; o.i, outer integument. Arrowheads indicate the *ANT* expression signals in the chalazal zone. Bars = 20 μm.
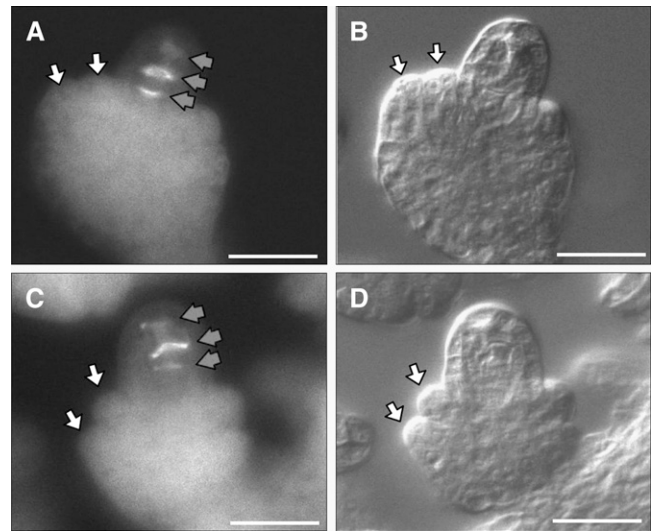

Figure 5. Meiosis in the Wild Type and the $mpk3^{+/-}$ $mpk6^{-/-}$ Mutant.

(A) and **(C)** Wide-field fluorescence microscopy of wild-type **(A)** and $mpk3^{+/-}$ $mpk6^{-/-}$ **(C)** ovules. Ovules were stained with aniline blue to detect callose accumulation. Callose deposition is shown as bright areas (indicated by gray arrows). In both wild-type and $mpk3^{+/-}$ $mpk6^{-/-}$ ovules, three bands of callose accumulation were visible, which mark the position of newly formed cell walls that divide the four meiotic nuclei into the tetrad.
(B) and **(D)** Nomarski images of the same wild-type **(B)** and $mpk3^{+/-}$ $mpk6^{-/-}$ **(D)** ovules to show the normal initiation of inner and outer integuments of the $mpk3^{+/-}$ $mpk6^{-/-}$ ovule at early stages.
White arrows indicate inner and outer integuments. Bars = 20 μm.

$mpk3^{+/-}$ $mpk6^{-/-}$ ovules, the enlargement of MMC and the formation of tetrad occurred normally. Staining with aniline blue confirmed the meiotic nature of the cell divisions of the MMC in the $mpk3^{+/-}$ $mpk6^{-/-}$ ovules (Figures 5C and 5D). Aniline blue stains callose, which marks the newly formed cell plate of the meiotically dividing MMC during megasporogenesis (Rodkiewicz, 1970). This result suggests that the female sterility of $mpk3^{+/-}$ $mpk6^{-/-}$ plants is due to a defect other than sporophytic control of megasporogenesis.

To determine if there are any defects associated with megagametogenesis, we examined ovules at different developmental stages by semithin sectioning. The developmental progression from tetrad degeneration to mononucleate embryo sac formation to vacuole-bearing four-nucleate embryo sac formation in $mpk3^{+/-}$ $mpk6^{-/-}$ plants is normal compared with wild-type ovules (Figures 6A to 6H). However, concomitant with the enlargement of the vacuole and the dissolving of nucellar layer at the micropylar end, the embryo sac shape was deformed in the mutant ovules. It was observed that the embryo sacs borne in the $mpk3^{+/-}$ $mpk6^{-/-}$ mutant ovules were forced out like a bubble or occasionally pinched into two segments. In addition, the integuments were not long enough to cover the micropylar end of the embryo sac (Figures 6H to 6K; see Supplemental Figure 2 online). By contrast, the wild-type embryo sac was enclosed by the integuments and was kidney shaped (Figure 6D).
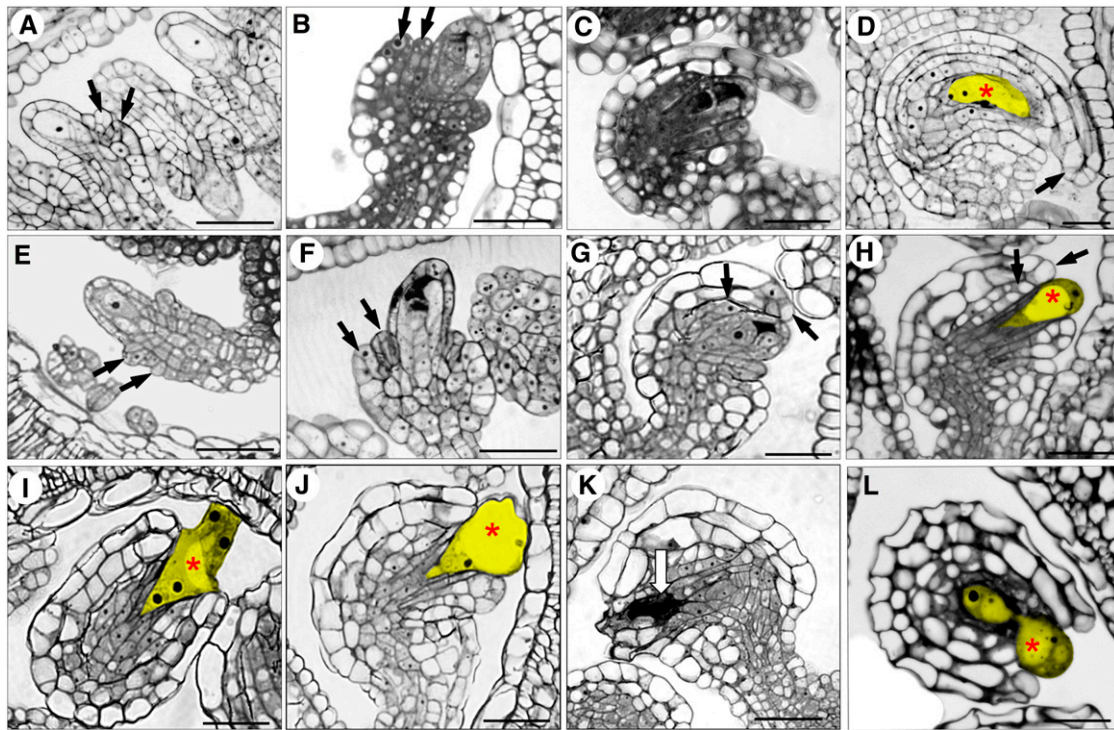
Figure 6. Semithin Sections of the Developing Wild-Type and *mpk3*$^{+/-}$ *mpk6*$^{-/-}$ Mutant Ovules.

(A) to **(D)** Wild-type ovules at stage 2-III **(A)**, stage 2-V **(B)**, stage 3-I **(C)**, and stage 3-IV **(D)**.
(E) to **(L)** *mpk3*$^{+/-}$ *mpk6*$^{-/-}$ mutant ovules at stage 2-III **(E)**, stage 2-V **(F)**, stage 3-I **(G)**, stage 3-IV (**[H]** to **[K]**), and beyond stage 3-VI **(L)**.
Black arrows indicate the tip of inner and outer integuments; red asterisks indicate the vacuole in the embryo sac; the white arrow indicates the degenerated embryo sac. Enlarging embryo sacs are highlighted by yellow color in **(D)**, **(H)** to **(J)**, and **(L)**. Bars = 20 μm. For more examples of developing embryo sacs in *mpk3*$^{+/-}$ *mpk6*$^{-/-}$, see Supplemental Figure 2 online.

The Development of Ovule Integuments at Later Stages Was Arrested in the *mpk3*$^{+/-}$ *mpk6*$^{-/-}$ Mutant

In wild-type ovules at stage 3-I (mononucleate embryo sac stage), the inner and outer integuments undergo active cell division and elongate rapidly to accommodate the rapidly enlarging embryo sac (Figure 6C). By stage 3-IV (the four-nucleate embryo sac stage), both inner and outer integuments envelop the nucellus with the micropylar end pointing ~90° away from the funiculus (Figure 6D). The initiation and early outgrowth of inner and outer integuments in *mpk3*$^{+/-}$ *mpk6*$^{-/-}$ ovules was normal (Figure 6E). However, the continual growth and the formation of curvature in the integuments were disrupted in the mutant (Figures 6H to 6L). The integuments were shorter and unable to extend beyond the nucellus, resulting in the exposure of the embryo sac (Figures 6H to 6J).

Alterations in cell size, cell number, or both can contribute to the variation of organ size. To investigate whether the shorter integuments in the *mpk3*$^{+/-}$ *mpk6*$^{-/-}$ mutant ovules were due to reduced cell size, cell division, or both, we measured the cell size and cell number in the outer integuments. In wild-type ovules, the cell size in the outer integuments was not uniform; the cells at the micropylar end were larger than those at the chalazal end. To avoid this size variation, we measured the cell size of the third through fifth cells from the micropylar end of the outside layer of outer integuments. As shown in Figure 7A, the average cell size in the *mpk3*$^{+/-}$ *mpk6*$^{-/-}$ mutant (175 μm^2) was slightly larger than that in the wild type (132 μm^2). This result suggests that the shorter integument in the *mpk3*$^{+/-}$ *mpk6*$^{-/-}$ mutant is not due to reduced cell expansion.

To determine if the smaller integument organ size in the *mpk3*$^{+/-}$ *mpk6*$^{-/-}$ mutant was due to a reduction in cell proliferation, we counted the cell numbers in the surface layer of outer integuments at stages 2-V and 3-IV. At stage 2-V, about the same number of cells was observed in the outer layer of the outer integuments in the *mpk3*$^{+/-}$ *mpk6*$^{-/-}$ mutant and wild-type ovules. However, at stage 3-IV, there were fewer cells in the outmost layer of the integument in the *mpk3*$^{+/-}$ *mpk6*$^{-/-}$ mutant ovules than that in the wild-type ovules (Figure 7B). It was also noted that there was no significant increase in cell number at stage 3-IV compared with stage 2-V in the *mpk3*$^{+/-}$ *mpk6*$^{-/-}$ mutant ovules, suggesting that the arrest of cell division is accountable for the abnormal integument morphogenesis in *mpk3*$^{+/-}$ *mpk6*$^{-/-}$ mutant ovules.

Physically Restricted Embryo Sacs in *mpk3*$^{+/-}$ *mpk6*$^{-/-}$ Plants Developed to Mature Stages

To determine the identity and developmental stage of the physically restricted embryo sacs in the *mpk3*$^{+/-}$ *mpk6*$^{-/-}$ ovules, we
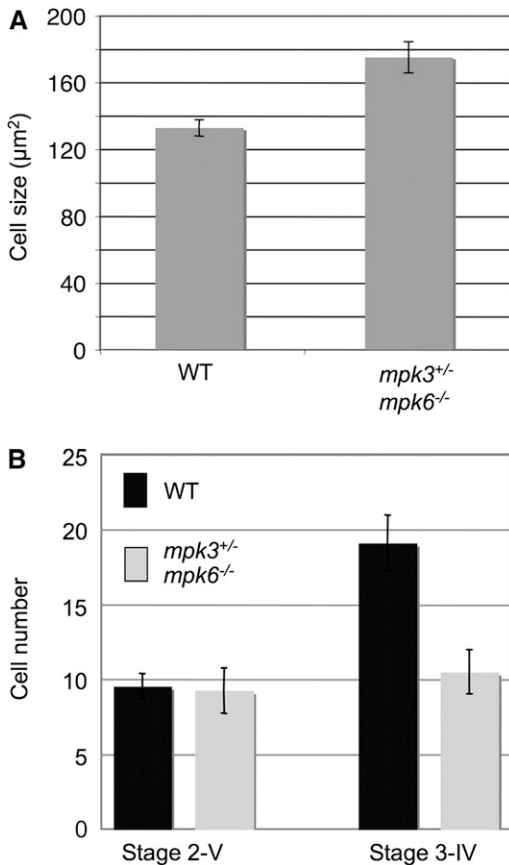
Figure 7. *MPK3* Is Haplo-Insufficient in Maintaining Integument Growth.

(A) Cell size measurement in the outside layer of outer integuments. Error bars represent SE ($n = 30$).

(B) Cell number count in the outside layer of outer integuments. At stage 2-V, there is no significant difference in the cell numbers between the wild type and $mpk3^{+/-}$ $mpk6^{-/-}$ mutant. At stage 3-IV, there are significantly fewer cells in the mutant integument than in the wild type. There is no significant increase in the cell numbers in the mutant integument at stage 3-IV compared with stage 2-V. Error bars represent SD ($n = 20$).

crossed the MET333 β-glucuronidase (GUS) marker line (Acosta-Garcia and Vielle-Calzada, 2004) into $mpk3^{-/-}$ $mpk6^{+/-}$ plants and generated MET333 $mpk3^{+/-}$ $mpk6^{-/-}$ plants. MET333 shows initial GUS expression at the four-nucleate embryo sac stage. At the eight-nucleate stage, MET333 expression is restricted to the young antipodal cells and the cellularizing egg apparatus. At maturity, the MET333 GUS expression was observed in the synergids, the egg cell, and the antipodals but not in the central cell (Acosta-Garcia and Vielle-Calzada, 2004). In the $mpk3^{+/-}$ $mpk6^{-/-}$ ovules, MET333 GUS activity was detected at both the chalazal and the micropylar ends of the ovules (Figure 8B), suggesting that the embryo sacs had developed beyond the four-nucleate stage in the $mpk3^{+/-}$ $mpk6^{-/-}$ plants, even though they were pinched into two segments. In the mature wild-type embryo sacs, the central cell with a large vacuole was easily visible (Figure 8A). These results suggest that the development of female game-

tophytes progress normally in the $mpk3^{+/-}$ $mpk6^{-/-}$ ovules. Female sterility of $mpk3^{+/-}$ $mpk6^{-/-}$ plants appears to be due to the physical restriction of the developing embryo sacs by the abnormal sporophytic integuments.

YDA Is the Potential Upstream MAPKKK of MPK3/MPK6 in Regulating Ovule Development

Recently, it was demonstrated that MPK3/MPK6 function downstream of MKK4/MKK5 and YDA (a MAPKKK) in coordinating the epidermal cell fate specification of stomata versus pavement cells (Bergmann et al., 2004; Wang et al., 2007a). *yda* homozygous mutant plants rarely survived to the flowering stage. Nt *MEK2* is the tobacco (*Nicotiana tabacum*) ortholog of *Arabidopsis MKK4* and *MKK5* (Yang et al., 2001; Ren et al., 2002). We have shown that basal level expression of *GVG*-Nt*MEK2^DD^*, a gain-of-function mutant of Nt MEK2, was able to rescue multiple growth
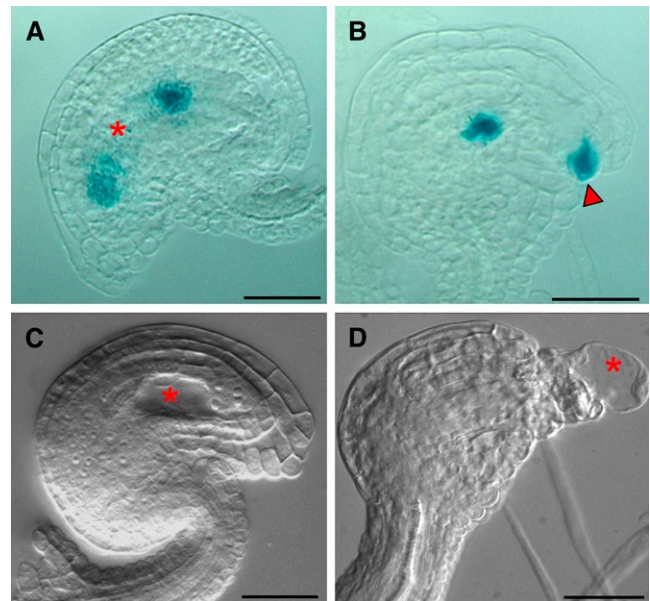

Figure 8. Embryo Sacs in $mpk3^{+/-}$ $mpk6^{-/-}$ Plants Develop to Mature Stage, and the Partially Rescued *yda* Plants Have Similar Restricted Embryo Sacs.

(A) and **(B)** Expression pattern of MET333, a female gametophyte development marker line, in the wild type and $mpk3^{+/-}$ $mpk6^{-/-}$ mutant.
(A) GUS staining of the MET333 reporter line in the wild-type ovules. At maturity, GUS expression is localized in the antipodals (chalazal end), the synergids, and the egg cell (micropyle end).
(B) GUS staining of the MET333 reporter line in the $mpk3^{+/-}$ $mpk6^{-/-}$ mutant ovules of the same stage. GUS staining signal is detected in both the chalazal and the micropyle ends, which is consistent with the pattern in a mature embryo sac, even though the embryo sac was pinched into two segments by the integuments and no central vacuole was visible.
(C) and **(D)** The Nomarski image of partial rescued *yda* mutant ovules.
(C) Control ovule development at stage 3-V in Nt MEK2^DD^ transgenic plants.
(D) Ovule development in Nt MEK2^DD^yda at a similar stage.
Red asterisks indicate vacuole in the embryo sac; red arrowhead indicates GUS staining signal in the micropyle end. Bars = 20 μm.

and developmental defects in *yda* (Wang et al., 2007a). *GVG-NtMEK2*^{DD}/*yda* has normal flower formation. However, the partially rescued *GVG-NtMEK2*^{DD}/*yda* is female sterile. Similar to that observed in the *mpk3*$^{+/-}$ *mpk6*$^{-/-}$ ovules, the integuments in the *GVG-NtMEK2*^{DD}/*yda* plants were shorter and unable to extend beyond the nucellus, resulting in the embryo sac being squeezed out (Figures 8C and 8D). This result suggests that YDA is likely to be the upstream MAPKKK of MPK3/MPK6 in ovule development.

MPK3 and MPK6 Are Both Expressed in the Developing Ovules

To determine the expression patterns of *MPK3* and *MPK6* during ovule development, we used RNA in situ hybridization and promoter:GUS reporter constructs. *MPK3* transcripts were detected broadly in the ovule primordia, ovule integuments, and carpels up to the mature stage (Figures 9A to 9F; see Supplemental Figure 3 online). Similar to *MPK3*, *MPK6* transcripts and promoter activity were detected broadly in the ovule primordia, ovule integuments, and carpels (Figures 9G to 9L). Expression of

MPK6 was also detected at the carpel margin before ovule primordia initiation (Figure 9G). The broad expression pattern of *MPK6* is consistent with a previous report (Bush and Krysan, 2007). The overlapping expression patterns of *MPK3* and *MPK6* during ovule development support the conclusion that MPK3 and MPK6 have overlapping functions in regulating ovule development based on genetic evidence.

DISCUSSION

In this report, we showed that *MPK3* and *MPK6* are essential to normal ovule development. In the absence of functional *MPK6*, *MPK3* is haplo-insufficient in maintaining female fertility. By contrast, heterozygous *MPK6* is sufficient to maintain female fertility when *MPK3* is not functional. We propose that the gene dosage–dependent activation of MPK3 and MPK6 and activation compensation of MPK6 in the absence of MPK3 might contribute to the novel haplo-insufficiency of *mpk3*$^{+/-}$ *mpk6*$^{-/-}$ in maintaining female fertility. Genetic analysis indicates that the female sterility in the *mpk3*$^{+/-}$ *mpk6*$^{-/-}$ plants is due to a sporophytic
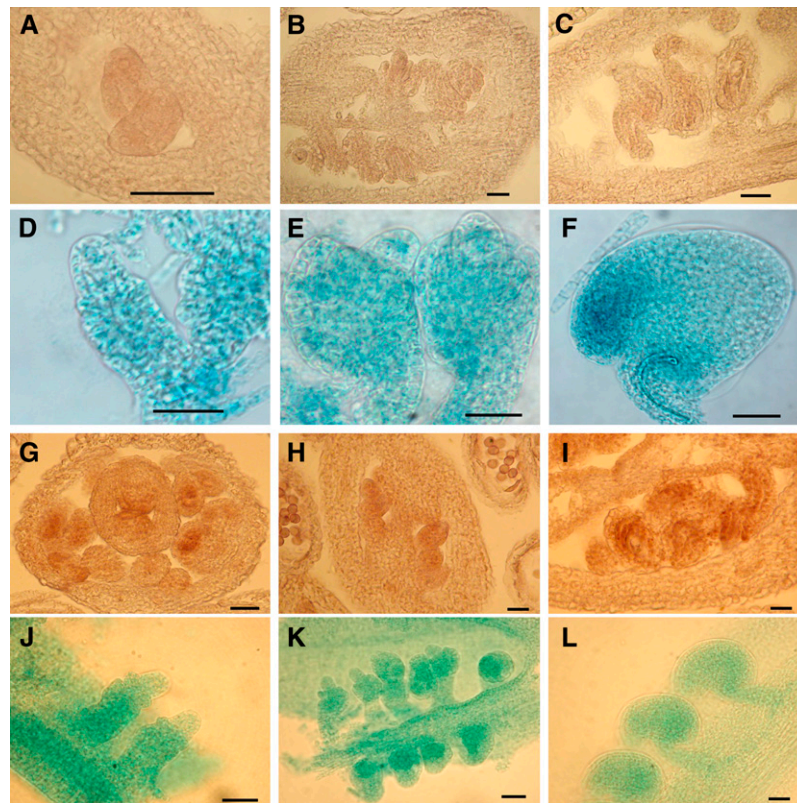

Figure 9. Expression Pattern of *MPK3* and *MPK6* during Ovule Development.

(A) to **(C)** Expression pattern of *MPK3* detected by in situ hybridization. MPK3 transcription pattern is shown for stage 2-I **(A)**, stage 2-V **(B)**, and stage 4-I **(C)** ovules. Sections were probed with *MPK3* antisense probe.
(D) to **(F)** *PMPK3:GUS* expression is shown for stage 2-II **(D)**, stage 2-V **(E)**, and stage 4-I **(F)** ovules.
(G) to **(I)** Expression pattern of *MPK6* detected by in situ hybridization. *MPK6* transcription pattern is shown at the carpel margin **(G)**, stage 2-I **(H)**, and stage 3-V **(I)** ovules. Sections were probed with *MPK6* antisense probe.
(J) to **(L)** *PMPK6:GUS* expression is shown for stage 2-II **(J)**, stage 2-IV **(K)**, and stage 3-V **(L)** ovules.
Bars = 20 μm.

defect. Further analysis indicates that MPK3 and MPK6 are essential in maintaining cell proliferation during integument development in ovules. The short integuments in the $mpk3^{+/-}$ $mpk6^{-/-}$ mutants failed to accommodate the developing embryo sac, which results in female sterility. Our work highlights the essential functions of a MAPK cascade in regulating ovule integument development.

As signaling molecules, potential roles of MPK3 and MPK6 in plant ovule development include (1) regulating the growth/morphogenesis of integuments after sensing a signal from the embryo sac, (2) coordinating the growth/morphogenesis of integuments after sensing a signal from neighboring sporophytic cells, and (3) controlling the cell division of integuments autonomously. It has long been speculated that active signaling events regulate the coordinated growth of the sporophytic integuments and the gametophytic embryo sac (Klucher et al., 1996; Acosta-Garcia and Vielle-Calzada, 2004; Yadegari and Drews, 2004). However, in $fem12$ or $fem16$ mutants, the integuments divide and elongate normally while no embryo sac forms, suggesting that integument development does not require a fully functional embryo sac (Christensen et al., 2002). In the wild type, the embryo sac undergoes rapid enlargement from stages 3-I to 3-IV; concomitantly, the ovule integuments divide and elongate rapidly to accommodate and fully enclose the growing embryo sac (Figures 6C and 6D). By contrast, the cell division of integuments at late stages is arrested in $mpk3^{+/-}$ $mpk6^{-/-}$ mutant ovules, suggesting that these two MAPKs are involved in promoting the cell division at this specific stage. Based on the fact that the cell division in other parts of the $mpk3^{+/-}$ $mpk6^{-/-}$ mutant plants is normal, we speculate that MPK3 and MPK6 are involved in transducing a signal originated either from embryo sac or from neighboring sporophytic cells to promote cell division/development in ovules.

In $mpk3^{+/-}$ $mpk6^{-/-}$ mutant plants, the megasporogenesis and megagametogenesis proceeded normally (Figures 5 and 6) and the female gametophyte identity was correctly established (Figures 8A and 8B). One interesting observation is that the embryo sacs in the $mpk3^{+/-}$ $mpk6^{-/-}$ mutant ovules were deformed; they were either forced out like a balloon with an angular chalazal end or pinched into two segments (Figures 6H to 6L; see Supplemental Figure 2 online). This is in sharp contrast with the kidney-shaped embryo sacs in the wild type (Figure 6D). As depicted in the diagram (Figure 10), the geometrical appearance of the embryo sacs is energetically unfavorable (Lecuit and Lenne, 2007), suggesting that there is a restrictive physical force being exerted on the growing embryo sac by the integuments of the mutant ovules. This observation indicates that the abnormal development of diploid sporophytic integuments results in the loss of the ability for the integuments to accommodate the rapid enlargement of the developing embryo sac in the $mpk3^{+/-}$ $mpk6^{-/-}$ ovules. The failure of sporophytic integuments to accommodate the developing embryo sac could therefore contribute to the female-sterile defects in the $mpk3^{+/-}$ $mpk6^{-/-}$ plants. Alternatively, it could be argued that the lack of complete coverage of the developing embryo sac could cause the sterile defect in the $mpk3^{+/-}$ $mpk6^{-/-}$ mutants. In wishbone flower (*Torenia fournieri*), the embryo sac is naturally half-exposed outside of the integuments, but the plant is fully fertile (Guilford and Fisk, 1951;
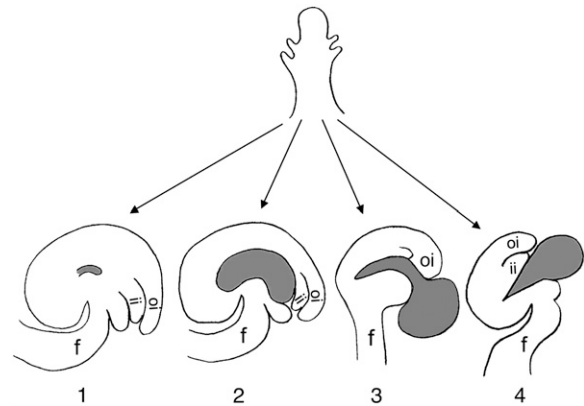

Figure 10. Diagram Depicting the Interactions between Sporophytic Ovule Integuments and Developing Female Gametophyte.

(1) As in *fem12*, female gametophyte development is arrested at early stage and no embryo sac formation occurs. However, the ovule integuments develop normally, suggesting that the development of ovule integuments does not require functional female gametophyte. (2) In contrast with (1), the wild type has a big enlarging embryo sac and the ovule integuments can sense and accommodate the existence of developing embryo sac. (3) As in *Torenia*, short ovule integuments do not fully enclose the developing embryo sac, resulting in the embryo sac being exposed. However, the partially exposed embryo sacs are still viable. (4) As in the $mpk3^{+/-}$ $mpk6^{-/-}$ mutant, the short integuments fail to accommodate the developing embryo sac, resulting in the physical restriction of female gametophyte and female sterility. oi, outer integument; ii, inner integument; f, funiculus. Gray highlights the developing embryo sac.

Higashiyama et al., 1997; Wallwork and Sedgley, 2000) (Figure 10), which could argue against the hypothesis that physical exposure causes the female sterility in $mpk3^{+/-}$ $mpk6^{-/-}$ plants. However, one should bear in mind that other mechanisms may have evolved in *Torenia* that allow its partially exposed and partially restricted embryo sac to be viable (Guilford and Fisk, 1951; Higashiyama et al., 1997; Wallwork and Sedgley, 2000).

Recent studies have highlighted the essential functions of MPK3 and MPK6 in signaling multiple growth and developmental processes. It was demonstrated that MPK3/MPK6 regulates embryo, stomata, inflorescence, and anther development (Bush and Krysan, 2007; Wang et al., 2007a). In this study, the unique haplo-insufficiency of MPK3 in the MPK6 mutant background helped us uncover a novel function of MPK3/MPK6 in ovule development. This opens up the interesting question of how the signaling specificity of MPK3/MPK6 is maintained in different growth and developmental pathways. In yeast and animal systems, multiple mechanisms exist for maintaining the signaling specificity of MAPK cascades, including (1) different cell types express distinct receptors and/or MAPK substrates, (2) quantitative differences in signaling strength/timing program distinct outcomes, (3) different combinations of signaling pathways are activated by distinct ligand-receptor pairs, (4) mechanisms that spatially restrict signaling by pathway-specific scaffold proteins or formation of complexes, and (5) cross-pathway suppression of downstream components (Widmann et al., 1999;

Chang and Karin, 2001; Vaudry et al., 2002; Morrison and Davis, 2003; Chou et al., 2004; Schwartz and Madhani, 2004; Kolch, 2005; Remenyi et al., 2005; Dard and Peter, 2006; Mor and Philips, 2006). Plants might employ similar mechanisms to maintain signaling specificity.

MPK3/MPK6 are known to assemble with different MAPKKKs to form different MAPK cascades. It has been shown that MPK3/MPK6 form a cascade with MKK4/MKK5 and MEKK1 in stress-responsive signaling pathways (Asai et al., 2002). The same MPK3/MPK6 can also form a cascade with MKK4/MKK5 and YODA in regulating stomatal development and patterning (Wang et al., 2007a). These results indicate that the same MAPK can function with different MAPKKKs and possibly different MAPKKs to convey different input signals. In addition, differential regulation by upstream components in a temporal- and spatial-specific fashion may play a critical role in maintaining the signaling specificity of the MPK3/MPK6 signaling cascade. For example, the YDA-MKK4/MKK5-MPK3/MPK6 cascade functions downstream of TMM (for Too Many Mouths) in regulating stomatal development and patterning in a cell-type or tissue-specific manner (Bergmann et al., 2004; Wang et al., 2007a). *TMM* is expressed specifically in the meristemoid mother cells, meristemoids, guard mother cells, or young guard cells but not in the pavement cells and the mesophyll cells. Similarly, MEKK1-MKK4/MKK5-MPK3/MPK6 was demonstrated to be downstream of FLS2 (for FLAGELLIN INSENSITIVE2) in response to the bacterial elicitor flg22 (Asai et al., 2002). The magnitude and duration of the MAPK activity are also known to contribute to the signaling specificity of the MAPK cascade (Widmann et al., 1999). Previously, we reported that MPK3 and MPK6 function together in regulating stomatal development as well. In the conditionally rescued $mpk3^{-/-}$ $mpk6^{-/-}$ seedlings, cotyledon epidermis is mostly composed of stomata (Wang et al., 2007a). However, no stomatal development defect was observed in $mpk3^{+/-}$ $mpk6^{-/-}$ plants. These results indicate that one copy of the *MPK3* gene is sufficient for normal stomatal development but not for ovule development, suggesting that a lower-strength MAPK signal is sufficient to maintain normal stomatal development. Differential thresholds could allow *MPK3/MPK6* to program a specific output and fine-tune the specificity of MAPK signaling.

Morphogenesis of the ovule integument requires coordinated cell division, cell expansion, and cell shape determination. In the $mpk3^{+/-}$ $mpk6^{-/-}$ mutants, the coordinated cell division, cell expansion, and cell shape determination were disrupted. The arrested cell division in the $mpk3^{+/-}$ $mpk6^{-/-}$ ovule integuments was partially compensated for by the enlargement of cell size (Figure 7). Frequently, irregular cell shapes were observed in the $mpk3^{+/-}$ $mpk6^{-/-}$ ovule integuments (Figure 6). Known mutants, such as *sin1/dcl1*, *sin2*, *tsl*, *seu*, and *lug*, have reduced integument outgrowth. Mutation of these genes also has a pleiotropic effect on other developmental processes, suggesting that a significant number of ovule developmental regulators are multifunctional and their specific biological functions are determined by the tissue context (Robinson-Beers et al., 1992; Roe et al., 1997; Broadhvest et al., 2000; Franks et al., 2002; Golden et al., 2002). At this stage, how MPK3 and MPK6 function together with these components is unknown. The defect of $mpk3^{+/-}$ $mpk6^{-/-}$ plants is mostly restricted to ovule development, as the mutants have normal stature and no defect in floral organ morphogenesis (Figure 1). Recently, it was demonstrated that the ERECTA gene families play essential functions in regulating ovule integument development in a dosage-sensitive manner (Pillitteri et al., 2007). Although the experimental evidence is still lacking, it is tempting to speculate that MPK3/MPK6 cascade might function downstream of ERECTA family receptor-like protein kinases in regulating intercellular interaction during ovule integument development.

METHODS

Plant Materials and Growth Conditions

Arabidopsis thaliana Columbia (Col-0) ecotype was used as the wild type. Null T-DNA insertion alleles of *MPK3* (At3g45640), *mpk3-1* and *MPK6* (At2g43790), *mpk6-1*, *mpk6-2*, and *mpk6-3* were described earlier (Liu and Zhang, 2004; Wang et al., 2007a). A second *MPK3* allele, *mpk3-DG*, was a fast neutron deletion mutant kindly provided by Brian Ellis (Miles et al., 2005). All three *mpk6* mutant alleles gave the same phenotype in either of the two *mpk3*$^{+/-}$ mutant allele backgrounds. Throughout the article, results from a cross of *mpk3-1* and *mpk6-3* are presented. The MET333 marker line was generously provided by Jean-Philippe Vielle-Calzada (Acosta-Garcia and Vielle-Calzada, 2004). After surface sterilization and imbibing at 4°C for 3 to 5 d, seeds were plated on half-strength Murashige and Skoog medium with 0.7% phytagar and appropriate antibiotics for selection. Plates were incubated in a tissue culture chamber at 22°C under continuous light (70 μE m^{-2} s^{-1}) for 7 d. Seedlings were then transplanted into soil and grow in the greenhouse with a 16-h-light/8-h-dark cycle.

Transgenic Plant Generation

To make the *MPK6* complementation construct, a 2834-bp fragment upstream of the ATG start codon of *MPK6* was amplified with MPK6-F1 (5′-TCTGAATTCGTCCGGTTACAGAGATCTCACAGA-3′) and MPK6-B1 (5′-TCTCCCGGGCATGACCGGTAAAGATGAAAGCTT-3′). This upstream sequence was then cloned into pCAMBIA3300 between *Eco*RI and *Sma*I. cDNA of MPK6 was amplified with cMPK6-F (5′-TCTCCCGGG-ATGGACGGTGGTTCAGGTCAACCG-3′) and cMPK6-NOSterminator-B (5′-CTCTCTAGAAATTCCCGATCTAGTAACATAGAT-3′) with the NOS terminator incorporated at the 3′ end. This cMPK6-NOS terminator fragment was then cloned into the *Sma*I and *Xba*I sites of pCAMBIA3300 to generate the final construct of *pCAMBIA3300-PMPK6:cMPK6-NOSter*. This construct was then introduced into *Agrobacterium tumefaciens* strain GV3101 by electroporation. *PMPK6:cMPK6* construct was transformed into *mpk3*$^{-/-}$ *mpk6*$^{+/-}$ plants by the floral dipping method (Clough and Bent, 1998). Basta-resistant transgenic plants were genotyped. Transgenic plants with *mpk3*$^{-/-}$ *mpk6*$^{+/-}$ background were pollinated with *mpk6*$^{-/-}$ pollen. In the F1 generation, all *mpk3*$^{+/-}$ *mpk6*$^{-/-}$ *PMPK6:cMPK6* plants were fertile, confirming that the *PMPK6:cMPK6* transgene was able to complement the sterile phenotype of *mpk3*$^{+/-}$ *mpk6*$^{-/-}$. For generating the *PMPK6:GUS* promoter fusion, the 2834-bp fragment upstream of ATG was cloned into the *Eco*RI site in pKUT593 (Shpak et al., 2004). Primers used for PCR amplification were MPK6-F1 (5′-TCTGAATTCGTCCGGTTACAGA-GATCTCACAGA-3′) and MPK6-B2 (5′-TCTGAATTCCATGACCGGTAAA-GATGAAAGCTT-3′).

Wounding Activation of MPK3 and MPK6

Plants of various phenotypes were selected from an F2 segregating population after genotyping. Leaves were wounded by punching out leaf discs using a cork borer (Zhang and Klessig, 1998). Samples from three

newly matured leaves were pooled to reduce leaf–leaf variation. After 10 min, leaf discs were quickly frozen in liquid nitrogen and used for protein extraction. In-gel kinase assay was performed according to Zhang and Klessig (1997). Ten micrograms of total protein was loaded onto each lane. At least three independent biological samples were examined with similar results.

Scanning Electron Microscopy and Semithin Sectioning

Plant samples were fixed in 4% formaldehyde, 0.25% glutaraldehyde, 0.01% Triton X-100, 100 mM sodium chloride, and 10 mM sodium phosphate, pH 6.8, for 2 h. The samples were then washed in phosphate buffer and deionized water. Secondary fixation was completed with 1% osmium tetroxide for 2 h. Samples prepared for scanning electron microscopy were then washed and dehydrated for critical point drying and sputter coated with platinum. Scanning electron microscopy images were collected using a Hitachi S4700 cold-cathode field-emission scanning electron microscope. Samples prepared for semithin sectioning were dehydrated and embedded in the Spurr's resin. Sections (2 to 3 μm) were prepared with a Leica Ultracut UCT ultramicrotome. The sections were stained in 0.05% toluidine blue.

Cell Size Measurement and Cell Number Counts

Images of semithin sections of ovules were used for cell size measurement. Cell size of the third through fifth cells from the distal end of the outside layer of outer integuments was measured with MetaMorph. Significance of difference was calculated using a Student's t test (P < 0.01; $n = 30$). Cleared ovules were used for cell number count. Cell number in the outer layer of outer integuments was counted from the distal ends (micropylar ends) to the proximal ends (chalazal ends). Significance of difference was calculated using a Student's t test (P = 0.01; $n = 20$).

In Situ RNA Hybridization

Developing flower buds were fixed in FAA (3.7% formaldehyde, 5% acetic acid, and 50% ethanol) and embedded in Paraplast (Sigma-Aldrich). Sections (10 to 12 μm) were prepared with a Spencer 820 microtome and mounted on Superfrost microscope slides (Fisher Scientific). To generate in situ probe, a 650-bp fragment of *INO* cDNA (25 to 675), a 670-bp fragment of *AINTEGUMENTA* cDNA (80 to 750), a 695-bp fragment of *MPK3* cDNA (1 to 695), and a 363-bp fragment of *MPK6* cDNA (864 to 1227) were cloned into pBluescript +. The resulting constructs were digested with *Xho*I or *Bam*HI to be used as template for synthesizing dioxygenin-labeled sense and antisense RNA probes. In situ RNA hybridization was performed according to Long et al. (1996) and Balasubramanian and Schneitz (2000).

GUS Staining

Gus staining of whole-mount ovules was performed as described (Vielle-Calzada et al., 2000). Dissected siliques were incubated in *GUS* staining buffer (10 mM EDTA, 0.1% Triton X-100, 2 mM potassium ferricyanide, 2 mM potassium ferrocyanide, 100 μg mL^{-1} chloramphenicol, and 1 mg mL^{-1} X-Gluc [Biosynth] in 50 mM sodium phosphate buffer, pH 7.0) for 6 h at 37°C. The siliques were then cleared in Hoyer's solution (Liu and Meinke, 1998), and the ovules were dissected out and observed on an Olympus IX-70 microscope equipped with Nomarski optics.

Aniline Blue Staining and Microscopy

Open siliques were fixed in acetic acid/ethanol (1:3) for 3 h and cleared with 70% ethanol. Ovules were then dissected out and mounted on the slides in a drop of decolorized 0.1% (w/v) aniline blue (100 mM K$_3$PO$_4$, pH 11, and 10% glycerol). Images were taken with an Olympus IX70 inverted microscope equipped with wide-field fluorescence optics.

Accession Numbers

Sequence data from this article can be found in the Arabidopsis Genome Initiative or GenBank/EMBL databases under the following accession numbers: MPK3 (At3g45640), MPK6 (At2g43790), ANT (At4g37750), and INO (At1g23420).

Supplemental Data

The following materials are available in the online version of this article.

  Supplemental Figure 1. Pollen Grains Produced from the *mpk3$^{+/-}$ mpk6$^{-/-}$* Mutant Plants Are Viable and Have Normal Development.

  Supplemental Figure 2. More Examples of Semithin Sections of Developing Ovules in the *mpk3$^{+/-}$ mpk6$^{-/-}$* Mutant as Shown in Figure 6.

  Supplemental Figure 3. Sense-Probe Control for in Situ RNA Hybridization of *MPK3*.

REFERENCES

Acosta-Garcia, G., and Vielle-Calzada, J.-P. (2004). A classical arabinogalactan protein is essential for the initiation of female gametogenesis in Arabidopsis. Plant Cell **16:** 2614–2628.

Asai, T., Tena, G., Plotnikova, J., Willmann, M.R., Chiu, W.-L., Gomez-Gomez, L., Boller, T., Ausubel, F.M., and Sheen, J. (2002). MAP kinase signalling cascade in Arabidopsis innate immunity. Nature **415:** 977–983.

Bajon, C., Horlow, C., Motamayor, J.C., Sauvanet, A., and Robert, D. (1999). Megasporogenesis in *Arabidopsis thaliana* L.: An ultrastructural study. Sex. Plant Reprod. **12:** 99–109.

Balasubramanian, S., and Schneitz, K. (2000). NOZZLE regulates proximal-distal pattern formation, cell proliferation and early sporogenesis during ovule development in *Arabidopsis thaliana.* Development **127:** 4227–4238.

Bergmann, D.C., Lukowitz, W., and Somerville, C.R. (2004). Stomatal development and pattern controlled by a MAPKK kinase. Science **304:** 1494–1497.

Broadhvest, J., Baker, S.C., and Gasser, C.S. (2000). SHORT INTEGUMENTS 2 promotes growth during Arabidopsis reproductive development. Genetics **155:** 899–907.

Bush, S.M., and Krysan, P.J. (2007). Mutational evidence that the Arabidopsis MAP kinase MPK6 is involved in anther, inflorescence, and embryo development. J. Exp. Bot. **58:** 2181–2191.

Chang, L., and Karin, M. (2001). Mammalian MAP kinase signalling cascades. Nature **410:** 37–40.

Chou, S., Huang, L., and Liu, H. (2004). Fus3-regulated Tec1 degradation through SCFCdc4 determines MAPK signaling specificity during mating in yeast. Cell **119:** 981–990.

Christensen, C.A., Gorsich, S.W., Brown, R.H., Jones, L.G., Brown, J., Shaw, J.M., and Drews, G.N. (2002). Mitochondrial GFA2 is required for synergid cell death in Arabidopsis. Plant Cell **14:** 2215–2232.

Christensen, C.A., King, E.J., Jordan, J.R., and Drews, G.N. (1997). Megagametogenesis in Arabidopsis wild type and the Gf mutant. Sex. Plant Reprod. **10:** 49–64.

Clough, S.J., and Bent, A.F. (1998). Floral dip: A simplified method for Agrobacterium-mediated transformation of *Arabidopsis thaliana.* Plant J. **16:** 735–743.

Dard, N., and Peter, M. (2006). Scaffold proteins in MAP kinase signaling: More than simple passive activating platforms. Bioessays **28:** 146–156.

Elliott, R.C., Betzner, A.S., Huttner, E., Oakes, M.P., Tucker, W.Q.J., Gerentes, D., Perez, P., and Smyth, D.R. (1996). AINTEGUMENTA, an APETALA2-like gene of Arabidopsis with pleiotropic roles in ovule development and floral organ growth. Plant Cell **8:** 155–168.

Franks, R.G., Wang, C., Levin, J.Z., and Liu, Z. (2002). SEUSS, a member of a novel family of plant regulatory proteins, represses floral homeotic gene expression with LEUNIG. Development **129:** 253–263.

Golden, T.A., Schauer, S.E., Lang, J.D., Pien, S., Mushegian, A.R., Grossniklaus, U., Meinke, D.W., and Ray, A. (2002). SHORT INTEGUMENTS1/SUSPENSOR1/CARPEL FACTORY, a Dicer homolog, is a maternal effect gene required for embryo development in Arabidopsis. Plant Physiol. **130:** 808–822.

Guilford, V.B., and Fisk, E.L. (1951). Megasporogenesis and seed development in *Mimulus tigrinus* and *Torenia fournieri.* Bull. Torrey Bot. Club **79:** 6–24.

Hamel, L.P., et al. (2006). Ancient signals: Comparative genomics of plant MAPK and MAPKK gene families. Trends Plant Sci. **11:** 192–198.

Higashiyama, T., Kuroiwa, H., Kawano, S., and Kuroiwa, T. (1997). Kinetics of double fertilization in *Torenia fournieri* based on direct observations of the naked embryo sac. Planta **203:** 101–110.

Huang, B.Q., and Russell, S.D. (1992). Female germ unit - Organization, isolation, and function. Int. Rev. Cytol. **140:** 233–293.

Ichimura, K., Shinozaki, K., Tena, G., Sheen, J., Henry, Y., Champion, A., Kreis, M., Zhang, S., and Hirt, H. (2002). Mitogen-activated protein kinase cascades in plants: A new nomenclature. Trends Plant Sci. **7:** 301–308.

Klucher, K.M., Chow, H., Reiser, L., and Fischer, R.L. (1996). The AINTEGUMENTA gene of Arabidopsis required for ovule and female gametophyte development is related to the floral homeotic gene APETALA2. Plant Cell **8:** 137–153.

Kolch, W. (2005). Coordinating ERK/MAPK signalling through scaffolds and inhibitors. Nat. Rev. Mol. Cell Biol. **6:** 827–837.

Lecuit, T., and Lenne, P.F. (2007). Cell surface mechanics and the control of cell shape, tissue patterns and morphogenesis. Nat. Rev. Mol. Cell Biol. **8:** 633–644.

Liu, C.M., and Meinke, D.W. (1998). The titan mutants of Arabidopsis are disrupted in mitosis and cell cycle control during seed development. Plant J. **16:** 21–31.

Liu, Y., and Zhang, S. (2004). Phosphorylation of 1-aminocyclopropane-1-carboxylic acid synthase by MPK6, a stress-responsive mitogen-activated protein kinase, induces ethylene biosynthesis in Arabidopsis. Plant Cell **16:** 3386–3399.

Long, J.A., Moan, E.I., Medford, J.I., and Barton, M.K. (1996). A member of the KNOTTED class of homeodomain proteins encoded by the STM gene of Arabidopsis. Nature **379:** 66–69.

Meister, R.J., Kotow, L.M., and Gasser, C.S. (2002). SUPERMAN attenuates positive INNER NO OUTER autoregulation to maintain polar development of Arabidopsis ovule outer integuments. Development **129:** 4281–4289.

Miles, G.P., Samuel, M.A., Zhang, Y., and Ellis, B.E. (2005). RNA interference-based (RNAi) suppression of AtMPK6, an Arabidopsis mitogen-activated protein kinase, results in hypersensitivity to ozone and misregulation of AtMPK3. Environ. Pollut. **138:** 230–237.

Misra, R.C. (1962). Contribution to the embryology of *Arabidopsis thaliana* (GAY & MONN.). Agra. Univ. J. Res. Sci. **11:** 191–199.

Mor, A., and Philips, M.R. (2006). Compartmentalized Ras/MAPK signaling. Annu. Rev. Immunol. **24:** 771–800.

Morrison, D.K., and Davis, R.J. (2003). Regulation of MAP kinase signaling modules by scaffold proteins in mammals. Annu. Rev. Cell Dev. Biol. **19:** 91–118.

Nakagami, H., Pitzschke, A., and Hirt, H. (2005). Emerging MAP kinase pathways in plant stress signalling. Trends Plant Sci. **10:** 339–346.

Pedley, K.F., and Martin, G.B. (2005). Role of mitogen-activated protein kinases in plant immunity. Curr. Opin. Plant Biol. **8:** 541–547.

Pillitteri, L.J., Bemis, S.M., Shpak, E.D., and Torii, K.U. (2007). Haploinsufficiency after successive loss of signaling reveals a role for ERECTA-family genes in Arabidopsis ovule development. Development **134:** 3099–3109.

Ray, A., Robinson-Beers, K., Ray, S., Baker, S.C., Lang, J.D., Preuss, D., Milligan, S.B., and Gasser, C.S. (1994). Arabidopsis floral homeotic gene BELL (BEL1) controls ovule development through negative regulation of AGAMOUS gene (AG). Proc. Natl. Acad. Sci. USA **91:** 5761–5765.

Reiser, L., Modrusan, Z., Margossian, L., Samach, A., Ohad, N., Haughn, G.W., and Fischer, R.L. (1995). The BELL1 gene encodes a homeodomain protein involved in pattern formation in the Arabidopsis ovule primordium. Cell **83:** 735–742.

Remenyi, A., Good, M.C., Bhattacharyya, R.P., and Lim, W.A. (2005). The role of docking interactions in mediating signaling input, output, and discrimination in the yeast MAPK network. Mol. Cell **20:** 951–962.

Ren, D., Yang, H., and Zhang, S. (2002). Cell death mediated by MAPK is associated with hydrogen peroxide production in Arabidopsis. J. Biol. Chem. **277:** 559–565.

Robinson-Beers, K., Pruitt, R.E., and Gasser, C.S. (1992). Ovule development in wild-type Arabidopsis and two female-sterile mutants. Plant Cell **4:** 1237–1249.

Rodkiewicz, B. (1970). Callose in cell walls during megasporogenesis in angiosperms. Planta **93:** 39–47.

Roe, J.L., Nemhauser, J.L., and Zambryski, P.C. (1997). TOUSLED participates in apical tissue formation during gynoecium development in Arabidopsis. Plant Cell **9:** 335–353.

Schneitz, K., Hulskamp, M., and Pruitt, R.E. (1995). Wild-type ovule development in *Arabidopsis thaliana*: A light microscope study of cleared whole-mount tissue. Plant J. **7:** 731–749.

Schwartz, M.A., and Madhani, H.D. (2004). Principles of MAP kinase signaling specificity in *Saccharomyces cerevisiae.* Annu. Rev. Genet. **38:** 725–748.

Shpak, E.D., Berthiaume, C.T., Hill, E.J., and Torii, K.U. (2004). Synergistic interaction of three ERECTA-family receptor-like kinases

controls Arabidopsis organ growth and flower development by promoting cell proliferation. Development **131:** 1491–1501.

Tena, G., Asai, T., Chiu, W.L., and Sheen, J. (2001). Plant mitogen-activated protein kinase signaling cascades. Curr. Opin. Plant Biol. **4:** 392–400.

Vaudry, D., Stork, P.J., Lazarovici, P., and Eiden, L.E. (2002). Signaling pathways for PC12 cell differentiation: Making the right connections. Science **296:** 1648–1649.

Vielle-Calzada, J.P., Baskar, R., and Grossniklaus, U. (2000). Delayed activation of the paternal genome during seed development. Nature **404:** 91–94.

Villanueva, J.M., Broadhvest, J., Hauser, B.A., Meister, R.J., Schneitz, K., and Gasser, C.S. (1999). INNER NO OUTER regulates abaxial- adaxial patterning in Arabidopsis ovules. Genes Dev. **13:** 3160–3169.

Wallwork, M.A.B., and Sedgley, M. (2000). Early events in the penetration of the embryo sac in *Torenia fournieri* (Lind.). Ann. Bot. (Lond.) **85:** 447–454.

Wang, H., Chevalier, D., Larue, C., Ki Cho, S., and Walker, J.C. (2007b). The protein phosphatases and protein kinases of *Arabidopsis thaliana.* In The Arabidopsis Book, C.R. Somerville and E.M. Meyerowitz, eds (Rockville, MD: American Society of Plant Biologists), doi/10.1199/tab.0106, http://www.aspb.org/publications/arabidopsis/.

Wang, H., Ngwenyama, N., Liu, Y., Walker, J.C., and Zhang, S. (2007a). Stomatal development and patterning are regulated by environmentally responsive mitogen-activated protein kinases in Arabidopsis. Plant Cell **19:** 63–73.

Widmann, C., Gibson, S., Jarpe, M.B., and Johnson, G.L. (1999). Mitogen-activated protein kinase: conservation of a three-kinase module from yeast to human. Physiol. Rev. **79:** 143–180.

Yadegari, R., and Drews, G.N. (2004). Female gametophyte development. Plant Cell **16:** S133–S142.

Yang, K.-Y., Liu, Y., and Zhang, S. (2001). Activation of a mitogen-activated protein kinase pathway is involved in disease resistance in tobacco. Proc. Natl. Acad. Sci. USA **98:** 741–746.

Yang, W.-C., and Sundaresan, V. (2000). Genetics of gametophyte biogenesis in Arabidopsis. Curr. Opin. Plant Biol. **3:** 53–57.

Zhang, S., and Klessig, D.F. (1997). Salicylic acid activates a 48-kD MAP kinase in tobacco. Plant Cell **9:** 809–824.

Zhang, S., and Klessig, D.F. (1998). The tobacco wounding-activated MAP kinase is encoded by *SIPK.* Proc. Natl. Acad. Sci. USA **95:** 7225–7230.

Zhang, S., and Klessig, D.F. (2001). MAPK cascades in plant defense signaling. Trends Plant Sci. **6:** 520–527.